MATERIAL OUTFLOWS FROM CORONAL INTENSITY "DIMMING REGIONS" DURING CORONAL MASS EJECTION ONSET

LOUISE K. HARRA

Mullard Space Science Laboratory, University College London, Holmbury St. Mary, Dorking, Surrey RH5 6NT, UK

AND

ALPHONSE C. STERLING[1,2]

NASA Marshall Space Flight Center, SD50/Space Science Department, Huntsville, AL 35812

ABSTRACT

One signature of expulsion of coronal mass ejections (CMEs) from the solar corona is the appearance of transient intensity dimmings in coronal images. These dimmings have generally been assumed to be due to discharge of CME material from the corona, and thus the "dimming regions" are thought of as an important signature of the sources of CMEs. We present spectral observations of two dimming regions at the time of expulsion of CMEs, using the Coronal Diagnostic Spectrometer (CDS) on the *SOHO* satellite. One of the dimming regions is at the solar limb and associated with a CME traveling in the plane of the sky, while the other region is on the solar disk and associated with an Earth-directed "halo" CME. From the limb event, we see Doppler signatures of $\approx$30 km s^{-1} in coronal (Fe XVI and Mg IX) emission lines, where the enhanced velocities coincide with the locations of coronal dimming. This provides direct evidence that the dimmings are associated with outflowing material. We also see larger ($\approx$100 km s^{-1}) Doppler velocities in transition region (O V and He I) emission lines, which are likely to be associated with motions of a prominence and loops at transition region temperatures. An "EIT wave" accompanies the disk event, and a dimming region behind the wave shows strong blueshifted Doppler signatures of $\approx$100 km s^{-1} in O V, suggesting that material from the dimming regions behind the wave may be feeding the CME.

Subject headings: Sun: corona — Sun: coronal mass ejections (CMEs) — Sun: transition region

1. INTRODUCTION

White-light coronagraphs, such as the Large Angle and Spectrometric Coronagraph (LASCO) instrument on the *SOHO* spacecraft, continue to provide invaluable information about coronal mass ejections (CMEs). Coronagraphs, however, are not able to observe the source of CMEs on the solar disk. Coronal observations of the source regions can be of great value in identifying Earth-directed CMEs, which tend to be the most important CMEs from a space weather standpoint (see, e.g., Brueckner et al. 1998; Webb et al. 2000). Such on-disk observations are also invaluable in determining the ultimate driving mechanism of CMEs, since they aid us in seeing the coronal structures involved in the eruptions and allow us to examine the underlying photospheric magnetic fields involved with the eruptions once the source regions are determined.

"Coronal dimmings" are a key coronal signature of the sources of CMEs. These are regions of the corona that undergo a drop in intensity at times roughly coincident with the times of CME onset. These dimmings can take many forms; e.g., Hansen et al. (1974) identified depleted regions at the solar limb. Some dimmings clearly result from movement of coronal structures (e.g., Rust & Hildner 1976). Rust (1983) called dimming areas seen on the disk in *Skylab* soft X-ray images "transient coronal holes." Hudson & Webb (1997) categorize various types of coronal dimmings. In this paper we discuss the nature of coronal dimmings for which there is no obvious mass motion observed in imaging instruments.

Researchers have often assumed that the coronal dimmings result from a depletion of coronal material (i.e., a decrease in density along the line of sight), even when no obvious moving

structure can be detected in images (e.g., Sterling & Hudson 1997; Gopalswamy & Hanaoka 1998; Thompson et al. 2000a; Hudson, Acton, & Freeland 1996), and that this material becomes part of the CME. Yet this explanation for the dimmings has not yet been unambiguously established. In addition to density, the intensity of coronal emission detected by soft X-ray and EUV telescopes also depends on temperature. Thus, in principle, the dimmings could be due to a dramatic change in the temperature of the emitting material. For example, the broadband soft X-ray telescope (SXT) on the *Yohkoh* spacecraft is sensitive to plasmas of temperatures $\gtrsim$2–3 MK (Tsuneta et al. 1991). Therefore, coronal material near 2 MK undergoing cooling at the time of a CME launch could result in dimming. For a narrowband instrument such as the EUV imaging telescope (EIT) on *SOHO* (Delaboudiniére et al. 1995), dimmings could result from either a significant cooling or heating of the coronal material.

In studies of two separate CME eruptions, Zarro et al. (1999), using SXT and EIT data, and Gopalswamy & Thompson (2000), using two different EIT filters, found that dimmings from the same events appear to be very similar in two different temperature regimes. This suggests that the dimmings are not the result of a change in temperature of the emitting regions, since, for example, a cooling of material from SXT temperatures might be expected to lead to an increase in intensity in the EIT 195 Å images as the material cools through 1.5 MK, the temperature at which the 195 Å images are most sensitive. These studies are not definitive, however, since a large enough temperature change could reduce intensity at both wavelengths, for example. In a similar type of study, Harrison & Lyons (2000), using image data from the Coronal Diagnostic Spectrometer (CDS) on *SOHO*, found that dimmings for a single event they observed were primarily confined to 10^6 K Mg IX

plasmas; they suggest that this material made up the bulk of the mass of the associated CME. Thus, several studies suggest that the dimming regions are the source of CME mass, although further confirmation of this is wanting.

In this paper we present the most direct evidence to date that the dimming regions result from mass loss, by observing Doppler motions of material leaving the regions as they dim. Our spectral data are from CDS, and we observe the Doppler shifts in two different events, one at the solar limb and one on the disk. Both episodes were associated with CMEs, and the implication is that the material outflows from the dimming regions directly fed the mass supply of the incipient CMEs.

2. OBSERVATIONS AND DATA ANALYSIS

Our observations include data from the CDS (Harrison et al. 1995), LASCO (Brueckner et al. 1995), and EIT (Delaboudiniére et al. 1995) on board the *SOHO* spacecraft.

2.1. *Limb Event*

Our first event occurred at the northwest limb on 1998 March 31, with dimming in coronal emission (Fe XVI) beginning just before 09:00 UT. A gap in the *GOES* 9 data between 08:30 and 09:45 UT prevents us from determining the soft X-ray classification of this event. We have CDS data covering the following emission lines: Ca X at 557.6 Å, Ne VI at 562.8 Å, He I at 584.3 Å, Fe XVI at 360.8 Å, Mg IX at 368.1 Å, and O V at 629.7 Å. We used the CDS study EJECT_V3, which resulted in a set of observations with $244'' \times 240''$ images "rastered" right to left (west to east), produced simultaneously in each spectral line. Each raster takes ≈15 minutes, and this is the cadence of our observations. We have images from 06:49 to 15:57 UT on 1998 March 31, which cover the period before, during, and after a CME was launched. All times used in this paper refer to the start of the rastering. LASCO first observed the CME in its C2 coronagraph at 11:04 UT and shows material being expelled from the west side of the Sun; Delannée (2000b) presents more details of the LASCO CME observations.

In this paper we concentrate on the analysis of the four strongest lines in the study: He I, O V, Mg IX, and Fe XVI, which have characteristic temperatures of 0.02, 0.25, 1, and 2 MK, respectively. For each spatial pixel in the resulting images we fitted the spectral lines with a Gaussian profile. We carried out fitting on all spatial pixels that have an intensity greater than 10% of the maximum intensity.

We examined the evolution of the erupting region using "difference images" in which we subtract an earlier image from a later image. Dimming associated with the eruption began no later than 08:26 UT. Figure 1 shows difference images with images at 08:58 UT subtracted from images at 09:14 UT for the four emission lines; this covers a time when the dimmings first become pronounced. The dimmings have a different character in the transition region images (He I and O V) from those in the coronal images (Mg IX and Fe XVI). In the coronal images, the dimmings are very extensive, with only limited regions of intensity enhancements. At the same time, the transition region images show much smaller dimming regions, and they also show strong looplike emission among the dimming regions. This strong emission is associated with a prominence that displays upward motion and velocity of roughly 30 km s^{-1} in He I. It is not clear, however, whether this prominence is actually ejected from the Sun (Delannée 2000b). Since the prominence is mainly cooler material, it is not apparent in the coronal images.
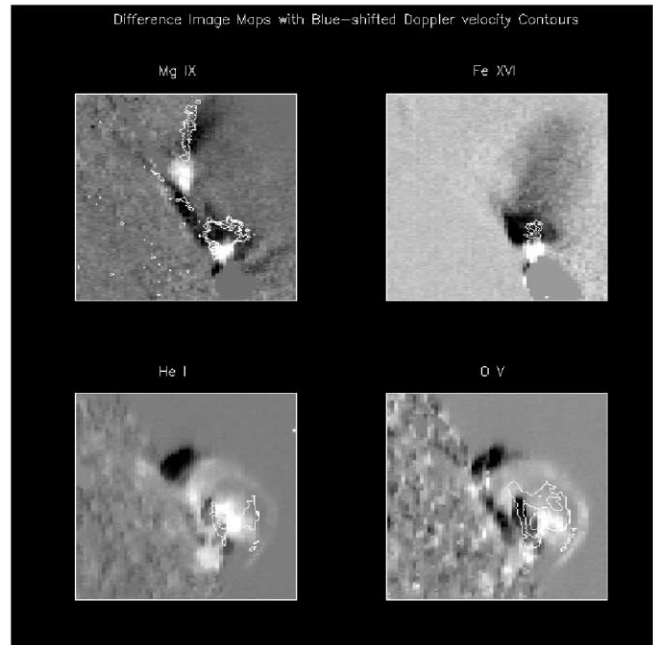

Fig. 1.—CDS difference images formed by subtracting images at 08:58 UT from images at 09:14 UT. *Top left*, Mg IX; *top right*, Fe XVI; *bottom left*, He I; *bottom right*, O V. The contours show blueshifted emission, with levels of −40, −30, and −20 km s^{-1} for Mg IX and Fe XVI and −130, −100, and −70 km s^{-1} for He I and O V.

We made velocity maps from the spectral information in the images by measuring the centroid shifts of the Gaussians fitted to each pixel. The "rest" wavelength was assumed to be that of the spectrum of all the pixels averaged over the entire raster scan. We have hence obtained a "relative" velocity. The errors on the spectral fitting are small (less than 5 km s^{-1}) as a result of the high count rate of the emission lines chosen. Figure 1 shows blueshifted contours in each of the four lines at the time of maximum blueshift. We did not detect strong redshifts in any of the emission lines at any time during the event.

We obtain a velocity image as a function of time over our sequence of rasters in each emission line. Figure 2 shows our resulting velocities, with the maximum blueshifts and redshifts shown for each raster. The strongest velocities are blueshifted (negative), although relatively weak redshifted (positive) velocities are apparent in the transition region lines. Overall, the largest motions are in the transition region lines, with maxima between −100 and −150 km s^{-1}. This is a factor of 2 larger than average active region transition region velocities previously determined from the CDS (approximately −50 km s^{-1}; e.g., Brekke, Kjeldseth-Moe, & Harrison 1997). Coronal velocities (Mg IX and Fe XVI) reach about −10 to −20 km s^{-1} beyond our region's ambient (background) level; while the magnitudes of the velocities are relatively small, we do expect that most of the motion would be normal to the line of sight for observations of this limb feature. By 13:00 UT, virtually all of the detected motions have slowed to ambient. Although this slowing could be due to actual slowing of the material detected by CDS, the presence of the CME suggests that this material was ejected. Thus, it is likely that the material left the CDS field of view (FOV) or became too tenuous for detection by CDS.

To determine where the regions of high velocity are located in relation to the dimming regions, we overlaid contours of the highest velocity regions onto the difference images in Figure 1. Both coronal ions show that the strong blueshifted emission
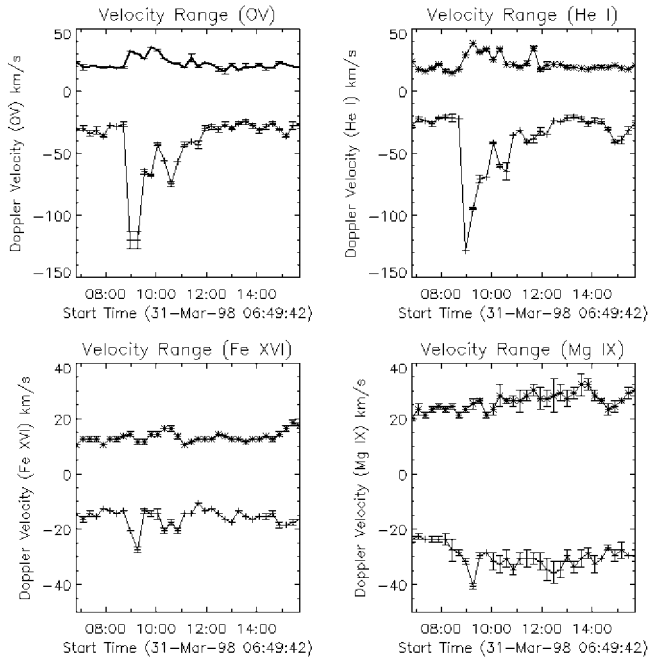
FIG. 2.—Range of velocities (the maximum redshifted and blueshifted velocities) in He I, O V, Fe XVI, and Mg IX, for each raster. The maximum blueshifted velocity (negative) is shown as a thin line and the maximum redshifted velocity (positive) as a thick line. The 1 σ standard deviations determined from the fits to the spectral lines are shown.
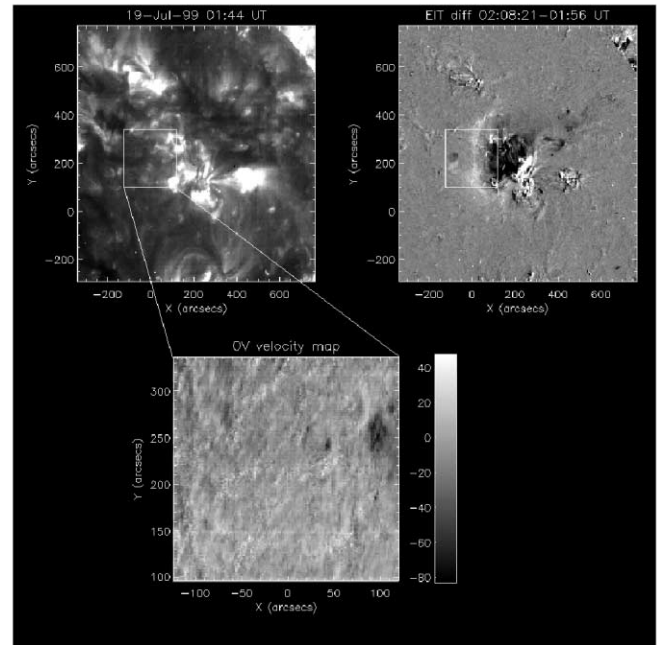

FIG. 3.—Upper left-hand EIT 195 Å image shows the active region of the disk event, with the CDS FOV indicated by the box. The upper right-hand EIT 195 Å image is a difference image that illustrates clearly the coronal wave, with the CDS FOV indicated by the box. The bottom image shows the velocity map in O V; the dark area on the right-hand edge indicates enhanced blueshifted emission, which coincides with the dimming behind the EIT wave in the upper right-hand image. The timing of the CDS raster is consistent with the enhanced blueshifts occurring behind the bright front of the EIT wave.

is cospatial with the strong dimming regions. This is our key result: it indicates the presence of strong mass motions in the corona localized to the dimming regions. Even for this limb event material is being ejected toward us with a velocity of 40 km s^{-1}.

Figure 1 also shows the highest velocity contours in the case of the cooler transition region lines (He I and O V). In contrast to the coronal emissions, the high velocities are not consistently cospatial with the dimming regions. Rather, they seem to be related more closely with the brighter features in the image, which largely represent highly activated prominence material along with evolving loops at transition region temperatures.

2.2. Disk Event

Our second event occurred in NOAA Active Region 8631 on 1999 July 19, starting at approximately 01:49 UT with a *GOES* C4 class flare. This event produced an EIT wave (e.g., Thompson et al. 2000b), with coronal dimmings appearing behind the wave; this contrasts with the limb event discussed above, which occurred without an obvious EIT wave. The LASCO C2 coronagraph observed a halo CME (e.g., Sterling & Hudson 1997) at 03:06 UT, which was likely to be associated with the event.

CDS runs a series of synoptic observations along the central meridian once per day. One of the scans overlapped the EIT wave and dimming just outside the active region. The upper left-hand side of Figure 3 shows the CDS FOV superimposed on an EIT 195 Å image of the region. In the upper right-hand panel of Figure 3, a difference image formed from EIT 195 Å images bracketing the time of the eruption shows the dimming region along with brighter emission associated with the flare and the EIT wave.

Our CDS data are from the CDS synoptic scans SYNOP_F, which use the following emission lines: Mg X at 624.8 Å, He I at 584.3 Å, Fe XVI at 360.8 Å, Mg IX at 368.1 Å, and

O V at 629.7 Å. SYNOP_F lasts for approximately 45 minutes, during which it scans a $244'' \times 240''$ FOV. We fitted the spectra for each spatial pixel in a similar way to the previous event. However, because of the low counts in the coronal lines, we concentrated only on the strong transition region O V emission line.

Figure 3 also shows the velocity map of O V. This shows unusually large Doppler velocities ($\lesssim$80 km s^{-1}) in the quiet Sun following the progression of the EIT wave through the CDS FOV. The exposure times of the raster location where the Doppler velocities are most pronounced ($80''-110''$ in the *x*-direction) cover 02:18–02:28 UT; the CDS raster carries on until 02:56 UT. The two EIT 195 Å images used in order to show the EIT wave as it commenced were taken at 01:56 and 02:08 UT. In the following difference image (02:20 and 02:08 UT), the bright ring has reached the left-hand edge of Figure 3, and most of the CDS FOV is encompassed by EIT dimming. Hence, the timings of the large CDS Doppler flows and the EIT dimmings are consistent.

3. DISCUSSION

We have provided the first Doppler velocity measurements of coronal intensity "dimming regions." For two different events, one at the limb and one on the disk, our results provide strong, direct evidence that the dimmings are a result of material outflows rather than a temperature effect or some other factor.

For the limb event, we see the dimmings most prominently in 1 and 2 MK coronal emission lines. Harrison & Lyons (2000), who also looked at a dimming region using CDS, found that the dimmings were substantial only at 1 MK, and not in the 1.3 MK Si x emission line. In our limb event we see a reduction in intensity of up to a factor of 6 for the Fe XVI emission line and up to a factor of 4 for the Mg IX emission

line. Thus, it appears as if the dimming we see includes higher temperature material than that observed in the event of Harrison & Lyons (2000).

Previous work on CME velocities has relied mainly on image intensity measurements against the sky plane (i.e., normal to the Sun-Earth line of sight), making velocity determinations difficult for CMEs originating on the disk. Our work provides a promising method for measuring velocities of front-side (Earth directed) CMEs; the EUV imaging spectrometer (EIS) device on the upcoming *Solar-B* mission should have adequate sensitivity and time cadence to utilize this method.

Our second event originated from the solar disk and produced an Earth-directed CME. The coronal flux detected by CDS, however, was too low for a detailed analysis of the coronal velocities, but we did detect high velocities in O v. This event showed dimming behind the bright edge of an EIT wave. Our results indicate that behind the bright front there was transition region material being removed with velocities up to 80 km s^{-1}. These Doppler signatures may represent motion of material expelled in the halo CME and resulting in the dimming.

Published accounts of EIT waves often report dimmings behind the waves (e.g., Thompson et al. 1999, 2000b; Delannée

2000a). Although flare-associated dimmings are detected more frequently than EIT waves, it seems plausible that the cause of the dimmings is the same in both cases. For example, a subset of these dimmings may result from an opening of field lines and subsequent material outflows associated with an erupting CME and flare, while in some of these cases an EIT wave results from, e.g., an impulse generated by the flare itself (Uchida 1968), or some aspect of the opening and evolving field lines (Delannée 2000a). Why the waves exist only in, or are detected only in, a subset of all eruptions is a mystery.

REFERENCES

Brekke, P., Kjeldseth-Moe, O., & Harrison, R. A. 1997, Sol. Phys., 175, 511
Brueckner, G. E., et al. 1995, Sol. Phys., 162, 357
———. 1998, Geophys. Res. Lett., 25, 3019
Delaboudiniére, J.-P., et al. 1995, Sol. Phys., 162, 291
Delannée, C. 2000a, ApJ, 545, 512
———. 2000b, J. Atmos. Sol.-Terr. Phys., 62, 1471
Gopalswamy, N., & Hanaoka, Y. 1998, ApJ, 498, L179
Gopalswamy, N., & Thompson, B. J. 2000, J. Atmos. Sol.-Terr. Phys., 62, 1457
Hansen, R. T., Garcia, C. G., Hansen, S. F., & Yasukawa, E. 1974, PASP, 86, 500
Harrison, R. A., et al. 1995, Sol. Phys., 162, 233
Harrison, R. A., & Lyons, M. 2000, A&A, 358, 1097
Hudson, H. S., Acton, L. W., & Freeland, S. L. 1996, ApJ, 470, 629

Hudson, H. S., & Webb, D. F. 1997, in Geophysical Monographs 99, Coronal Mass Ejections, ed. N. Crooker, J. Joselyn, & J. Feynman (Washington: AGU), 27
Rust, D. M. 1983, Space Sci. Rev., 34, 21
Rust, D. M., & Hildner, E. 1976, Sol. Phys., 48, 381
Sterling, A. C., & Hudson, H. S. 1997, ApJ, 491, L55
Thompson, B. J., Cliver, E. W., Nitta, N., Delannée, C., & Delaboudiniere, J.-P. 2000a, Geophys. Res. Lett., 27, 1431
Thompson, B. J., et al. 1999, ApJ, 517, L151
Thompson, B. J., Reynolds, B., Aurass, H., Gopalswamy, N., Gurman, J. B., Hudson, H. S., Martin, S. F., & St. Cyr, O. C. 2000b, Sol. Phys., 193, 161
Tsuneta, S., et al. 1991, Sol. Phys., 136, 37
Uchida, Y. 1968, Sol. Phys., 4, 30
Webb, D. F., Cliver, E. W., Crooker, N. U., St. Cyr, O. C., & Thompson, B. J. 2000, J. Geophys. Res., 105, 7491
Zarro, D. M., et al. 1999, ApJ, 520, L139